Current Biology, Volume *23*

Supplemental Information

An AP2 Transcription Factor Is Required for a Sleep-Active Neuron to Induce Sleep-like Quiescence in *C. elegans*

Michal Turek, Ines Lewandrowski, and Henrik Bringmann

Supplemental Information Inventory

Supplemental Figures
Figures S1 relates to Figure 2
Figures S2 relates to Figure 3
Figures S3 relates to Figure 4
Supplemental Experimental Procedures
Supplemental Movies
Movie 1 relates to Figure 1
Movie 2 relates to Figure 1
Movie 3 relates to Figure 3
Movie 4 relates to Figure 4
Supplemental References

Supplementary Figure S1:

A

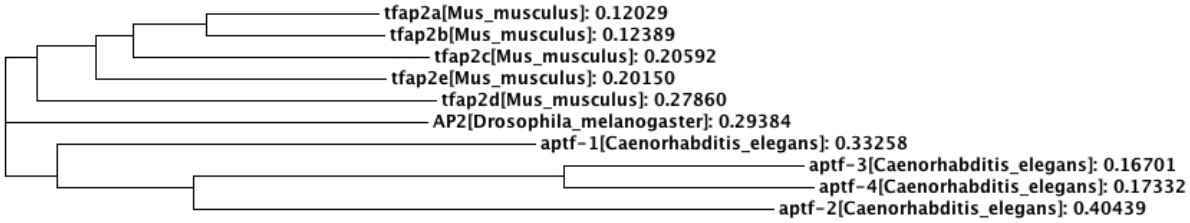

B

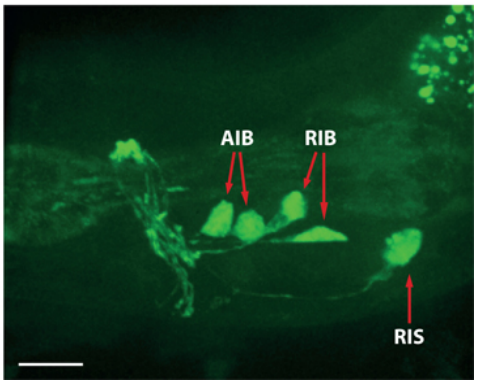

Fig. S1. Distance phylogram and expression of *aptf* genes in *C. elegans*. *aptf-1* is one of four *aptf* genes in *C. elegans* and is expressed in AIB, RIB, and RIS. **A** *aptf-1* is most similar to vertebrate *AP2* genes. *aptf* genes appear to have diverged independently of vertebrate *AP2* genes. The phylogenetic tree was calculated with ClustalW2, accession numbers/fosmid names: *tfap2a*[*Mus_musculus*] (NP_035677), *tfap2b*[*Mus musculus*] (NP_033360), *tfap2c*[*Mus musculus*] (NP_033361), *tfap2d*[*Mus musculus*] (NP_694794), *tfap2e*[*Mus musculus*] (NP_945198), *AP2*[*Drosophila melanogaster*] (NP_649336), *aptf-1*[*Caenorhabditis elegans*] (K06A1.1), *aptf-2*[*Caenorhabditis elegans*] (Y62E10A.17b), *aptf-3*[*Caenorhabditis elegans*] (F28C6.2), *aptf-4*[*Caenorhabditis elegans*] (F28C6.1). **B** Expression of *aptf-1* analyzed with a *gfp*-tagged fosmid. Spinning disc image of transgenic animals stably transformed with a fosmid containing a *gfp*-tagged version of *aptf-1*. The transcription factor was visible from L1 to adults in AIBs, RIBs, and RIS. Shown is an L4 worm, scale bar is 10µm.

Supplementary Figure S2:

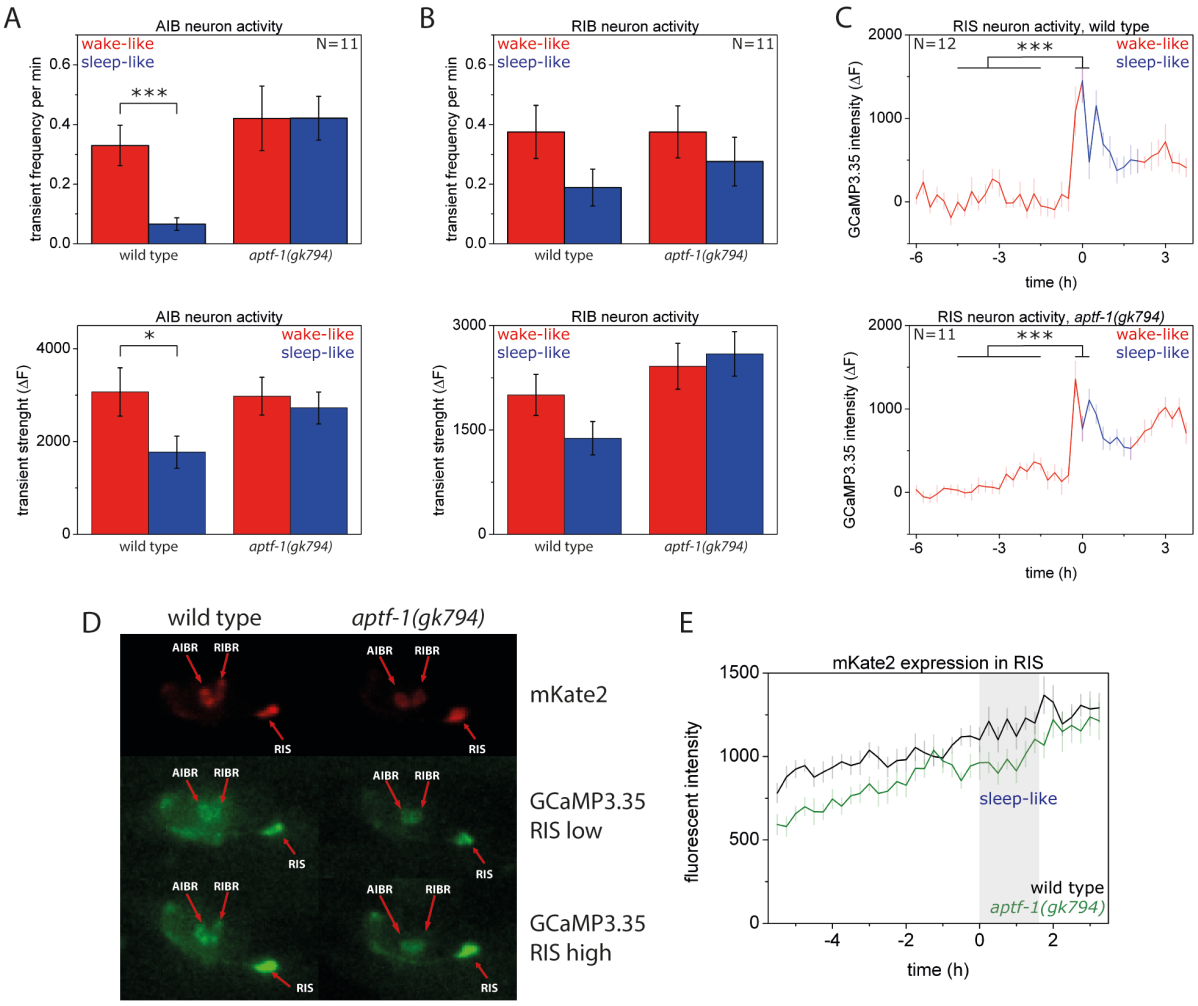

Fig. S2. Calcium imaging in *aptf-1*-expressing neurons: adjustment of GCaMP expression levels in *aptf-1* mutant worms. (**A-C**) The experiments are similar to those shown in Figure 3, except that worms homozygous for *goeIs118* were used. (**A**) Calcium transient frequency and intensity in AIB showed a reduced activity in this neuron during sleep-like behavior that depended on *aptf-1*. (**B**) Calcium transient frequency and intensity in RIB showed reduced activity during sleep-like behavior that partially depended on *aptf-1*. (**C**) Averaged calcium activity of RIS across time showed that RIS was most active during the transition from wake-like (red) to sleep-like (blue) behavior. RIS still activated at the onset of the sleep-like period in *aptf-1* mutant worms. (**D-E**) Signal quality and expression levels related to calcium imaging that is presented in Figure 3C. (**D**) The *aptf-1* promoter expresses calcium indicators strongly allowing reliable

calcium imaging. Sample images show the image quality of the focus plane containing RIS. Shown are the mKate2 expression that served as an expression control, the GCaMP expression during relative inactivity of RIS, and the GCaMP expression during RIS activation. (**E**) Expression in RIS in worms that are homozygous for *goeIs118* is similar to expression in RIS in worms that are heterozygous for *goeIs118* and mutant for *aptf-1*. Shown is the mKate2 signal during late L1 wake-like and sleep-like behavior. Expression is only 15% lower in *aptf-1* compared with wild type. Error bars are s.e.m.

Supplementary Figure S3:

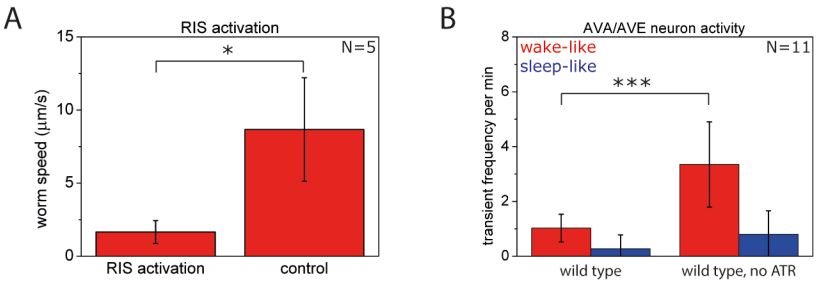

Fig. S3. ChR activation of RIS and command interneuron activity during ChR activation of *aptf-1*-expressing neurons. (**A**) Blue-light illumination was restricted to a region that was containing the RIS cell body but that was not containing AIB or RIB. As a control, an area close to the worm but not covering any ChR expressing neuron was illuminated. Control illumination did not cause any detectable behavioural response. Worm speed was measured at the position of the grinder. The reduction of speed upon RIS illumination was significant according to a Wilcoxon Signed Ranks test with $p < 0.05$. **(B)** *aptf-1*-expressing neurons were activated using ChR and command neuron activity was measured simultaneously using GCaMP calcium imaging. Channelrhodopsin-based activation of *aptf-1*-expressing neurons reduced calcium transient frequencies in AVA/AVE during wake-like behavior significantly according to a t-test with $p < 0.001$. Error bars are s.e.m.

Supplementary Methods:

Genetic screening

We performed a genetic screen by looking through existing mutants. We chose one allele for every gene for which a mutant was available from the Caenorhabditis Genetics Center (CGC), University of Minnesota, in January 2009. This selection resulted in 4000 strains that were obtained from the CGC. The worms were grown on standard 6cm NGM plates seeded with *E. coli* OP50 until the plates contained a population of about 400-600 worms of mixed developmental stages. Two individuals visually inspected the mixed populations independently for an absence of immobile worms. We found one mutant strain, VC1669 that both individuals scored to have no immobile animals in the mixed population. The population contained, however, worms that were not pumping.

Worm maintenance and strains

C. elegans was maintained on Nematode Growth Medium (NGM) plates seeded with *E. coli* OP50 as described [1]. Additional to the strains screened, the following strains and alleles were used:

N2: wild type

HBR16: *goeIs5[pnmr-1::SL1-GCaMP3.35-SL2::unc-54-3'UTR, unc-119(+)]*.

HBR227: *aptf-1(gk794)*.

HBR232: *aptf-1(tm3287)*.

HBR255: *aptf-1(gk794), unc-119(ed3), goeEx152[paptf-1::aptf-1::aptf-1-3'UTR; unc-119(+)]*.

HBR423: *goeIs91[wTRG5_09318202437763223_E07_K06A1-1.1_WRM0640B_F12--S0001_pR6K_Amp_2xTY1ce_EGFP_FRT_rpsl_neo_FRT_3xFlagd[29470..30845]--unc-119-Nat]*.

HBR437: *goeIs72[paptf-1::d1GFP::aptf-1-3'UTR; unc-119(+)]*.

HBR438: *aptf-1(gk794), goeIs72[paptf-1::d1GFP::aptf-1-3'UTR; unc-119(+)]*.

HBR498: *aptf-1(gk794), goeIs5[pnmr-1::SL1-GCaMP3.35-SL2::unc-54-3'UTR, unc-119(+)]*.

HBR543: *goeIs118[paptf-1::SL1-GCaMP3.35-SL2::mKate2-aptf-1-3'UTR; unc-119(+)]*.

HBR546: *goeIs102[paptf-1::ChR2::mKate2-aptf-1-3'UTR; unc-119(+)]*.

HBR555: *aptf-1(gk794), goeIs102[paptf-1::ChR2::mKate2-aptf-1-3'UTR; unc-119(+)]*.

HBR556: *aptf-1(gk794), goeIs118[paptf-1::SL1-GCaMP3.35-SL2::mKate2-aptf-1-3'UTR; unc-119(+)]*.

HBR667: *aptf-1(gk794), unc-119(ed3), goeIs173[pnpr-9::aptf-1::unc-54-3'UTR; unc-119(+)]*.

HBR740: *aptf-1(gk794), unc-119(ed3), goeEx291[psto-3::aptf-1-SL2::mKate2-unc-54-3'UTR; unc-119(+)]*.

HBR741: *aptf-1(gk794), unc-119(ed3), goeEx292[lim6int4::aptf-1-SL2::mKate2-unc-54-3'UTR; unc-119(+)]*.

HBR742: *goeIs5[pnmr-1::SL1-GCaMP3.35-SL2::unc-54-3'UTR, unc-119(+)]*, *goeIs102[paptf-1::ChR2::mKate2-aptf-1-3'UTR; unc-119(+)]*.

CB156: *unc-25(e156)*.

HBR743: *unc-25(e156), goeIs102[paptf-1::ChR2::mKate2-aptf-1-3'UTR; unc-119(+)]*.

VC461: *egl-3(gk283)*.

HBR650: *egl-3(gk283), goeIs102[paptf-1::ChR2::mKate2-aptf-1-3'UTR; unc-119(+)]*.

The deletion alleles *aptf-1(gk794)* (Caenorhabditis Genetics Center) and *aptf-1(tm3287)* (National Bioresource Project for the Experimental Animal "Nematode *C. elegans*") were backcrossed ten times against N2 to generate HBR227 and HBR232, respectively. These backcrossed strains were the basis for all experiments other than the screen. During backcrossing, the genotype was followed by PCR in each generation. Primers to detect the *aptf-1* deletions using a three primer PCR were:

48_VC1669_fwd:

5'-CGACAATCTTCCCAAAGACC-3'

49_VC1669_rev:

5'-CGGATCGATTGCTAGAGAGG-3'

50_N2_aptf1_fwd:

5'-GCTTGGACGGCTTTAGTTGA-3'

Three primer PCR resulted in the following product lengths:

wild type: 304 bp

aptf-1(gk794): 412 bp

aptf-1(tm3287): 581 bp

Molecular biology and transgenic strain generation

All constructs were cloned using the Gateway Multisite Gateway system (Invitrogen). All PCR-cloned pENTRY clones that were made with BP reactions and all constructs obtained from LR reactions were sequenced for verification.

aptf-1 promoter:

The *aptf-1* promoter was obtained by amplification of 1.5kb of the 5' region of *aptf-1* using PCR with genomic N2 DNA as a template. The primers containing *att* sites that were used were:

52_APTF_5'_fwd_B4:

5'-GGGGACAACTTTGTATAGAAAAGTTGAAACCTATTGCACATGTCTTGC-3'

53_APTF_5'_rev_B1R:

5'-GGGGACTGCTTTTTTGTACAAACTTGTCTGCAGTATCTGCATTTTTT-3'

aptf-1 coding region:

The *aptf-1* coding region including all introns was obtained by PCR amplification with genomic N2 DNA as a template. The primers containing *att* sites that were used were:

54_APTF_fwd_B1:

5'-
GGGGACAAGTTTGTACAAAAAAGCAGGCTATGTTCAACCGTAAACTCATGG-3'

55_APTF_rev_B2:

5'-
GGGGACCACTTTGTACAAGAAAGCTGGGTTTATCTCCAGACATTTTGAGAA-3'

aptf-1 3'UTR:

The *aptf-1* 3'UTR was obtained by amplification of 0.3 kb downstream of *aptf-1* using PCR with genomic N2 DNA as a template. The primers containing *att* sites that were used were:

56_APTF_3'_fwd_B2R

5'-GGGGACAGCTTTCTTGTACAAAGTGGTTACGCTTTGTCTTCTTGTTGA-3'

57_APTF_3'_rev_B3

5'-GGGGACAACTTTGTATAATAAAGTTGATTTCAGCAATTGGCTCATTTT -3'

To generate *goeIs5* we used pENTRY clones containing the *nmr-1* promoter and *unc-54* 3' UTR that were both a gift from Bill Schafer. For neuron-specific rescue experiments we used the following promoters: For expression in AIB we used a *npr-9* promoter that was a gift from Mario de Bono and *unc-54* 3' UTR. For expression in RIB, we used 970bp upstream of *sto-3* and the *unc-54* 3' UTR. For expression in RIS, we used an intron of *lim-6* that also causes expression in AVL[2] and the *unc-54* 3' UTR. The intron has been described as the third intron of *lim-6*[2]. This corresponds to intron four according to Wormbase release WS238 and we thus named it *lim-6int4*[3].

GCaMP3.35, d1GFP, Channelrhodopsin2, and mKate2:

GCaMP3.35 was used as described[4]. d1GFP, Channelrhodopsin2, and mKate2-*aptf-1-3'UTR* were computer designed: the coding regions were codon-optimized for expression in *C. elegans,* synthetic introns were added and DNA constructs were synthesized by a commercial supplier[5].

gfp-tagged *aptf-1* fosmid:

The fosmid *wTRG5_09318202437763223_E07_K06A1-1.1_WRM0640B_F12--S0001_pR6K_Amp_2xTY1ce_EGFP_FRT_rpsl_neo_FRT_3xFlagd[29470..30845]--unc-119-Nat* containing *gfp*-tagged *aptf-1* was a gift from M. Sarov and was previously described[6].

Transformation

Transgenic strains were generated using microparticle bombardment using *unc-119(ed3)* rescue as a selection[7, 8]. Strains were crossed using standard procedures. The presence of the *aptf-1* deletion was verified by PCR for all *aptf-1* mutant strains generated. For *aptf-1* rescue experiments with the endogenous *aptf-1* promoter, we bombarded the DNA construct directly

into *aptf-1(gk794), unc-119(ed3)* worms. For neuron-specific rescue experiments for *aptf-1* we injected the DNA constructs directly into *aptf-1(gk794), unc-119(ed3)* worms. Constructs for RIS and RIB rescue were made with SL2 mKate2. Every individual worm that was taken for analysis was checked for expression in the neuron of interest. Worms that did not express the array in the neurons of interest were discarded. Only few animals could be used for rescue testing in RIB, because only four out of 81 worms tested actually expressed the array in RIB.

DIC imaging and analysis of sleep-like behavior

All long-term imaging experiments were carried out in agarose microcompartments as described before[9]. Briefly, eggs were placed together with *E. coli* OP50 as a food source into agarose microcompartments that were cast using a PDMS stamp. Worms were imaged in DIC optics and filmed using time-lapse movies with 5s interval or burst type movies every 15 minutes for 20 seconds with 2frames/s. For nose speed measurements, the nose was tracked manually.

Calcium imaging

Calcium imaging was performed similar as described before using GCaMP3.35 and coexpression of mKate2 as an expression control[4]. Calcium imaging was performed using an Andor iXon (512 x 512 pixels) EMCCD camera and LED illumination (CoolLed) using standard GFP and Texas Red filter sets (Chroma). Exposure time was 5-20ms and allowed imaging of moving worms without blurring. The LED was triggered using the TTL “fire” signal of the EMCCD camera to illuminate only during exposure. LED intensity was in the range of 15-30%. EM gain was between 50 and 250. The illumination did not cause bleaching or any detectable behavioral changes. All calcium-imaging experiments were performed in agarose microcompartments. Typically, about 10-15 individuals were cultured in individual microcompartments that were in close vicinity. Animals were typically filmed in a “burst” mode, that means the worms were filmed repeatedly every 30 minutes for about 2 minutes with a framerate of 0.5-2/s. Multiple animals were processed in parallel by repeatedly visiting the individual compartments using an automatic stage (Prior Proscan2/3) set to low acceleration speeds. Before each fluorescent measurement, a brief DIC movie was taken to assess the developmental stage and behavioral state. Worms that were pumping with their pharynx were scored as being in the wake-like state.

AVA imaging

nmr-1 expresses in AVA, AVD, AVE, RIM, AVG, and PVC[10]. AVA and AVE were so close to each other that we could not always separate their signals. Because AVA and AVE are strongly connected via gap junctions and because they both are required for backwards movement, we measured a combined AVA/AVE signal. AVA/AVE intensities were extracted from the dataset by using a threshold. First all peak activities were extracted from the animal. Then, the calcium transient peaks were each assigned manually to their respective neurons. AVA/AVE showed the strongest activation transients during L1 of all neurons expressing GCaMP3.35 in this transgene, and was thus chosen as readout for command neuron activity. The background was determined as the average intensity below the threshold, and was subtracted. The dataset was visually inspected to ensure that all transients extracted were derived from AVA/AVE and to check that AVA/AVE activation always correlated with a backwards movement. *aptf-1* mutants showed a slight general increase of AVA/AVE transient frequency and amplitude. Consistent with this, *aptf-1* showed a slightly increased reversal frequency. The protocol for imaging AVA/AVE transients was filming individual worms every 30 minutes for 100 seconds with a frame rate of 2/s.

Imaging of *aptf-1*-expressing neurons

We used *goeIs118[paptf-1::SL1-GCaMP3.35-SL2::mKate2-aptf-1-3'UTR; unc-119(+)]* for calcium imaging of *aptf-1*-expressing neurons. In the *aptf-1* mutant background, expression from *goeIs118* was approximately twice as high compared with wild type, as measured by mKate2 fluorescence. We thus used worms homozygous for *goeIs118* as a wild type control, and worms heterozygous for *goeIs118* for *aptf-1* mutant worms. We made *aptf-1* mutants that were heterozygous *goeIs118* worms by mating *aptf-1* mutant males that were heterozygous for *goeIs118* with *aptf-1* mutants. For the analysis only F1 hermaphrodites were used. Based on mKate2 expression, expression from heterozygous *goeIs118* in *aptf-1* mutants was only 15% lower compared with homozygous *goeIs118* wild type. We calculated the calcium transient changes as deltaF/F to compensate for changes in baseline fluorescence[11].

Calcium transients in AIB and RIB were analyzed using a threshold. Transient peaks were extracted and were manually assigned to either AIB or RIB. Because RIS was difficult to keep in focus in moving worms, we took z stacks through the animal using a Prior Nanoscan Z. For analysis, first the z frame that contained RIS was selected manually and then the neuron was

cut out using a semiautomatic Matlab routine. For all neurons a suitable background area was selected manually in each frame and its intensity was subtracted from the intensity of the neuron.

Mechanical stimulation

Mechanical stimulation using dish tapping was carried out similar as described previously, except that a stronger tapper was used[4]. Briefly, a piston that was driven by an electromagnet stimulated the worms. The piston with the electromagnet was placed into a custom made aluminum holder and fixed to the microscope stage. A dish containing the worms was placed onto the same holder so that the piston hit the dish in the plane of the coverslips/worms. Image acquisition and tapping were shuttered so that the movement caused by the tapping did not blur the image. We used a Kuhnke H62 magnet. The protocol was repeated every 30 minutes with 10 seconds filming without stimulation (2frames/second), 10 seconds filming with 20 taps (2frames/second), 10 seconds filming without stimulation (2 frames/ second), and 180 seconds filming without stimulation (0.5 frames/second). We used a 10x lens plus an additional 1.5x lens. The field of view allowed the observation of four L1 larvae in neighboring compartments per experiment simultaneously. The experiment was performed three times. We selected one time point during wake, one at the onset of sleep when RIS activity was high, and one time point during the second half of sleep-like behavior when RIS was low for analysis.

Channelrhodopsin experiments

Channelrhodopsin experiments were performed inside agarose microcompartments. Hermaphrodite mother worms were grown on medium that was supplemented with 0.2mM all trans Retinal (Sigma). Eggs from these mothers and food from the same plates were placed into microcompartments without any further Retinal supplementation. Worms were stimulated with an LED of 490nm with about 0.36 mW/mm^2 as measured with a light voltmeter. To illuminate RIS only, we used 1000x magnification and closed the field aperture in the fluorescence illumination path as much as possible. This resulted in a restriction of the area illuminated by blue light to a spot was about 15µm in diameter. L1 wake-like worms were placed into microfluidic compartments and worms were then moved manually by moving the stage, and blue light was turned on and off manually. Using this setup, we illuminated an area starting from the second half of the terminal bulb of the pharynx that extended 15 µm towards the posterior. Because the RIS cell body is located ventral to the posterior bulb of the pharynx, and AIB and

RIB are anterior to the terminal bulb of the pharynx, this setup likely illuminated only the RIS cell body but excluded the majority of the RIS process and also excluded AIB and RIB. To test whether stray light emerged from the 15-µm spot and caused nonspecific ChR activation we illuminated an area close to the worm's head that did not include RIS.

Spinning disc imaging

Spinning disc imaging was performed with an Andor Revolution spinning disc system using a 488nm laser, a Yokogawa X1 spinning disc head, a 100x oil objective and an iXon EMCCD camera. Z stacks were taken and a maximum intensity projection calculated.

Neuron identification

Neurons expressing *aptf-1* were identified in HBR437 (*goeIs72[paptf-1::d1GFP::aptf-1-3'UTR; unc-119(+)]*) using a combination of spinning-disc microscopy and DIC microscopy. The neurons were identified based on the position of their nuclei as seen in DIC and the morphology of their processes as seen in GFP spinning disc microscopy. Additional to the strong expression in AIB, RIB and RIS we saw weak expression in ALM and in an unidentified tail neuron.

Neuron ablation

Neurons were ablated similar to previously described[12]. We used a 355nm laser focused to a near-diffraction limited spot (Rapp Opto, DPSL-355/14, direct coupling). We performed all ablations at 1000x magnification in a *goeIs118[paptf-1::SL1-GCaMP3.35-SL2::mKate2-aptf-1-3'UTR; unc-119(+)]* background to identify the neurons of interest. We identified and ablated neurons in late embryos using mKate2 fluorescence without using anesthetics. We verified ablation of neurons using mKate2 and GCaMP3.35 fluorescence and discarded worms that showed unspecific laser damage or worms in which the neurons of interest were not successfully ablated. We treated mock-ablated worms like ablated worms except that they were not irradiated[12].

Statistics

Statistical tests used were Wilcoxon Signed Paired Ranks test using Origin software. Error bars are s.e.m.

Description of supplementary videos:

Video S1. *aptf-1* mutants lack locomotion shutdown during sleep-like behavior.

The video shows wake-like and sleep-like behavior in wild type and *aptf-1* mutants. L1 larvae were cultured in agarose hydrogel microcompartments together with bacterial food. During sleep-like behavior in wild type, feeding stopped and the worms were largely immobile. During-sleep-like behavior in *aptf-1* mutants, feeding also stopped but the worms continued to be mobile. Images were taken with DIC optics and are displayed two times faster. Microcompartment size was 190µm x 190µm.

Video S2. Command interneuron activity is shut down during sleep-like behavior in wild type, but not in *aptf-1* mutants.

The video shows calcium transients in the command interneuron AVA/AVE during wake-like and sleep-like behavior in wild type and *aptf-1* mutants. L1 larvae were cultured in agarose hydrogel microcompartments together with bacterial food. During sleep-like behavior in wild type, AVA/AVE calcium transients were largely absent and worms were immobile. During-sleep-like behavior in *aptf-1* mutants, AVA/AVE calcium transients continued during the sleep-like behavior as defined by the absence of feeding. Images were taken with widefield epifluorescence microsopy and are displayed eight times faster. Microcompartment size was 190µm x 190µm.

Video S3. RIS activates during periods of reduced mobility at the onset of sleep-like behavior.

The video shows calcium transients in *aptf-1*-expressing neurons during the transition from wake-like to sleep-like behavior in wild type. L1 larvae were cultured in agarose hydrogel microcompartments together with bacterial food. At the transition from wake-like to sleep-like behavior, periods of mobility and periods of reduced mobility alternated. During this time, bouts of reduced activity always coincided with RIS activation transients. Nose speed and RIS intensity are displayed in the plot to illustrate their correlation. Images were taken with widefield epifluorescence microsopy and are displayed two times faster. Microcompartment size was 190µm x 90µm.

Video S4. Optogenetic activation of *aptf-1*-expressing neurons triggers acute, *aptf-1*-dependent immobility and cessation of pumping.

L1 larvae were cultured in agarose hydrogel microcompartments together with bacterial food. *aptf-1*-expressing neurons were activated during wake-like behavior using blue light. Blue light stimulation caused immobility and cessation of feeding in wild type, but not in *aptf-1* mutants. In *aptf-1* mutants, blue light stimulation rather caused an increase in mobility. Images were taken with DIC optics and are displayed two times faster. The light stimulus period is indicated by a blue dot. Microcompartment size was 190µm x 190µm.

Supplemental references

1. Brenner, S. (1974). The genetics of Caenorhabditis elegans. Genetics *77*, 71-94.
2. Hobert, O., Tessmar, K., and Ruvkun, G. (1999). The Caenorhabditis elegans lim-6 LIM homeobox gene regulates neurite outgrowth and function of particular GABAergic neurons. Development *126*, 1547-1562.
3. wormbase (WS238). http://www.wormbase.org/species/c_elegans/gene/WBGene00002988.
4. Schwarz, J., Lewandrowski, I., and Bringmann, H. (2011). Reduced activity of a sensory neuron during a sleep-like state in Caenorhabditis elegans. Curr Biol *21*, R983-984.
5. Redemann, S., Schloissnig, S., Ernst, S., Pozniakowsky, A., Ayloo, S., Hyman, A.A., and Bringmann, H. (2011). Codon adaptation-based control of protein expression in C. elegans. Nat Methods *8*, 250-252.
6. Sarov, M., Murray, J.I., Schanze, K., Pozniakovski, A., Niu, W., Angermann, K., Hasse, S., Rupprecht, M., Vinis, E., Tinney, M., et al. (2012). A genome-scale resource for in vivo tag-based protein function exploration in C. elegans. Cell *150*, 855-866.
7. Wilm, T., Demel, P., Koop, H.U., Schnabel, H., and Schnabel, R. (1999). Ballistic transformation of Caenorhabditis elegans. Gene *229*, 31-35.
8. Praitis, V., Casey, E., Collar, D., and Austin, J. (2001). Creation of low-copy integrated transgenic lines in Caenorhabditis elegans. Genetics *157*, 1217-1226.
9. Bringmann, H. (2011). Agarose hydrogel microcompartments for imaging sleep- and wake-like behavior and nervous system development in Caenorhabditis elegans larvae. J Neurosci Methods *201*, 78-88.
10. Brockie, P.J., Madsen, D.M., Zheng, Y., Mellem, J., and Maricq, A.V. (2001). Differential expression of glutamate receptor subunits in the nervous system of Caenorhabditis elegans and their regulation by the homeodomain protein UNC-42. J Neurosci *21*, 1510-1522.
11. Kerr, R.A. (2006). Imaging the activity of neurons and muscles. WormBook, 1-13.
12. Fang-Yen, C., Gabel, C.V., Samuel, A.D., Bargmann, C.I., and Avery, L. (2012). Laser microsurgery in Caenorhabditis elegans. Methods in cell biology *107*, 177-206.